

Melt Reaction in Blends of Poly(3-hydroxybutyrate) (PHB) and Epoxidized Natural Rubber (ENR-50)

H. K. Lee,¹ J. Ismail,¹ H. W. Kammer,² M. A. Bakar¹

¹School of Chemical Sciences, Universiti Sains Malaysia, 11800 Minden, Penang, Malaysia

²University of Halle, Mansfelder Str. 28, D-01309 Dresden, Germany

Received 16 October 2003; accepted 14 April 2004

DOI 10.1002/app.20808

Published online in Wiley InterScience (www.interscience.wiley.com).

ABSTRACT: Melt reaction in blends comprising immiscible biopolymer, poly(3-hydroxybutyrate) (PHB), and epoxidized natural rubber with 50 mol percent level of epoxidation (ENR-50), prepared by solvent-casting, has been studied. Differential scanning calorimetry (DSC) technique was used to measure the heat of reaction under isothermal annealing. The heat of reaction increases with respect to PHB and ENR-50 content as long as they constitute the dispersed phases and exhibits a maximum at about 50% PHB. A reaction mechanism comprising degradation of PHB chains to shorter chains bearing carboxyl end groups that subsequently react with epoxide group of the ENR-50 is proposed, providing the basis for kinetic analysis and determination of parameters that characterize the melt reaction. Two-phase morphologies, formed in the blends upon melting of PHB,

transform within minutes to homogeneous phase as observed under optical polarizing microscope. The two glass transition temperatures observed at -18.4 and 1.2°C for blends are associated, respectively, with immiscible ENR-50 and PHB phases. After annealing at 190°C an inward shift was observed, gradually closing in with increasing annealing time, and eventually merging into a single transition. This is an indication of progressive change in miscibility of the blends, as an effect of the melt reaction. FTIR spectra provide further evidence that supports the ring opening reaction of the epoxide group by the carboxyl group. © 2004 Wiley Periodicals, Inc. *J Appl Polym Sci* 95: 113–129, 2005

Key words: melt; blends; morphology; epoxidized natural rubber; poly(3-hydroxybutyrate)

INTRODUCTION

Poly(3-hydroxybutyrate) (PHB), an aliphatic polyester produced via bacterial fermentation process, is a biodegradable and biocompatible thermoplastic. However, it has two drawbacks. First, it degrades at temperatures slightly above its melting point, producing shorter chains with carboxyl chain ends.¹ This gives PHB a narrow window of thermal processing. Second, its high crystallinity makes it brittle, giving rise to inferior mechanical properties. Continuous efforts have, ever since, been focused on finding ways to improve the properties, and blending PHB with other polymers provides a potential solution.

Epoxidized natural rubber, ENR, is a new natural rubber modified by way of epoxidation, wherein the double bonds of the isoprene units have been replaced by epoxide groups.² While epoxidation is a random process, the degree of epoxidation can be conveniently controlled. Besides improved properties, ENR possesses epoxide group, which is reactive towards carboxyl group.^{3–5} In blends of PHB/ENR-50 such a re-

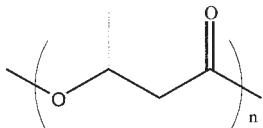
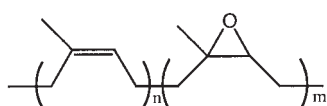
action involving the carboxyl end group of degraded PHB and the epoxide group of ENR is expected and may affect chemical and physical, as well as structural, changes at the interfaces of the immiscible PHB and ENR phases. Indeed, the phenomenon opens up a new scope of research and applications for PHB and ENR that merit further study. There have been reports on studies involving PHB with polymers having almost similar structure, for example poly(ethylene oxide),^{6–7} poly(methylene oxide),⁸ and poly(vinyl methylene oxide)⁹ in blends with PHB; none has so far been reported on PHB/ENR blends.

A preliminary study of the glass transition temperature conducted in our laboratory showed that blends of PHB and ENR possess two distinct values that, after annealing at temperatures above 184°C , have shifted inward as the annealing time was increased and eventually merged into a single transition.¹⁰ Since then we have started investigation on the reactions of PHB and ENR blends in melt phase. Being an incompatible blend system, the reactions will be confined to a highly viscous environment at the interfacial region of the immiscible phases. As a result, we anticipate interesting changes in the structure, morphology, and compatibility of the PHB/ENR blends that will give rise to new polymers with a wide range of properties. In this article, we present a study of the melt reactions in blends comprising PHB and ENR with 50 mol %

Correspondence to: J. Ismail (dchem@usm.my).

Sponsor: Universiti Sains Malaysia; contract grant number: Short Term Grant No. 304/P.Kimia/634066.

TABLE I
Characteristics of Purified PHB and ENR-50

Polymer	Structural formula	M_w (M_n)	T_g (°C)	Source
PHB		268000 (220000)	-1.0	Aldrich Chemical Co.
ENR-50		294000 (180000)	-18.0	Guthrie Polymer Sdn. Bhd.

epoxidation level, denoted here as ENR-50. In addition, we also highlight evidence of compatibility, an important consequence of the melt reaction and a crucial factor that would determine the phase behavior, morphologies, and properties of the blends.

EXPERIMENTAL

Materials

ENR (50 mol % epoxidized, denoted as ENR-50) was supplied by Guthrie Polymer Sdn Bhd Malaysia (Negeri, Sembilan) and purified before use. The purification steps involved dissolution of the rubber in chloroform, followed by filtration, and finally precipitation in methanol. PHB was purchased from Aldrich Chemical (Penang) and purified in the same way as described for ENR-50. Detail specifications of the two polymers after purification are given in Table I.

Preparation of blends

Blends PHB/ENR-50 comprising 20/80, 30/70, 40/60, 50/50, 60/40, 70/30, and 80/20 by weight were prepared by solvent-casting from 1% (w/w) solution of PHB/ENR-50 in chloroform, followed by evaporation at room temperature for 24 h, and finally drying under vacuum at 40°C for 48 h. Solvent-casting technique is chosen in this study to ensure homogeneous distribution of the two immiscible PHB and ENR-50 phases. Dried membrane of each composition was reduced to fine size, whenever possible, and mixed thoroughly to ensure reproducibility of samples used in the DSC experiments.

DSC experiments

Thermal analysis was carried out using Perkin-Elmer Differential Scanning Calorimetry, Pyris-6 (Shelton,

CT). The following thermal programs were carried out in this study.

Isothermal melt reaction

A 10 mg sample was heated under nitrogen atmosphere at 20°C/min from room temperature to 184°C, held isothermally (also referred to as annealing in this article) to allow melt reaction until completion by monitoring the thermogram output. This procedure was repeated for other reaction temperatures: 187, 190, 193, 196, and 199°C, respectively, using a new sample each time. The heating rate was chosen to ensure equilibrium between the sample and the programmed temperature as well as uniform distribution of heat throughout the sample.

Glass transition temperature, T_g

A 10 mg sample was heated under nitrogen atmosphere from room temperature to 190°C, allowed to anneal for 1 min before quenching to -70°C, held for 1 min, and finally heated again to 190°C. A heating of 20°C/min was used in this experiment. This procedure was repeated for other annealing times, 4 and 8 min respectively, using a new sample each time. Liquid nitrogen was used as coolant.

Characterization

Spectroscopic analysis of PHB/ENR-50 was carried out using Perkin-Elmer 2000 FTIR on ATR mode on samples treated according to glass transition temperature thermal procedure to look for evidence of reaction.

A Nikon Ellipse E600 (Japan) polarizing light microscope equipped with a Linkam hot stage (UK) was used to view changes in morphologies of PHB/

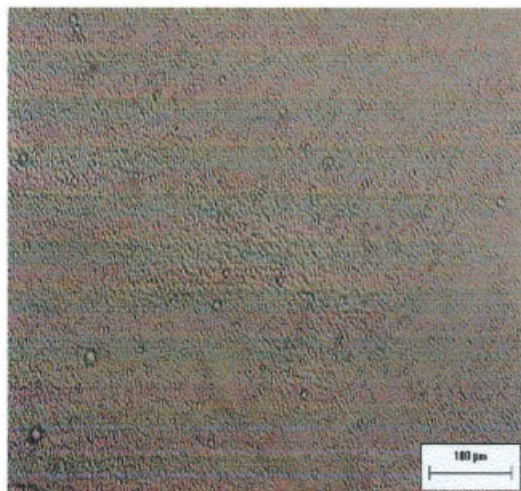
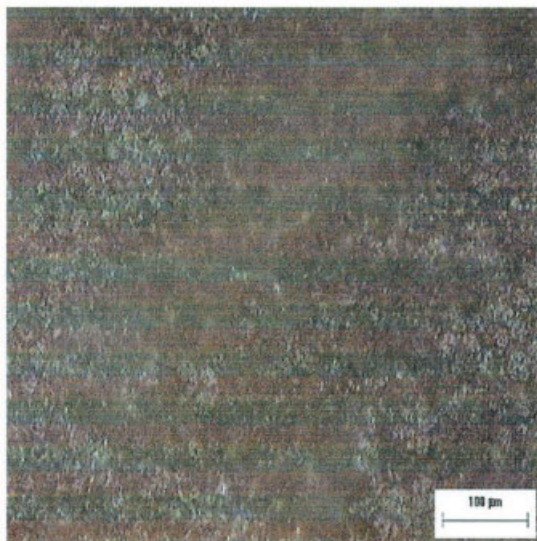
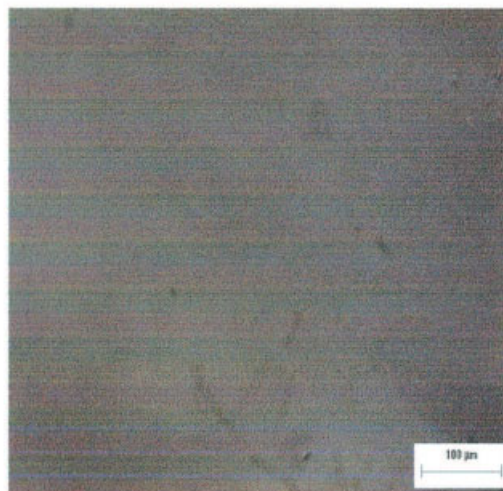
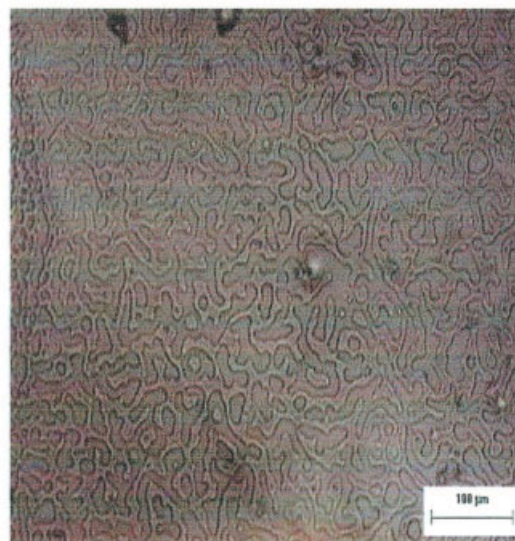
(a) Morphology of as prepared membrane**(i) PHB/ENR-50 (30/70)****(ii) PHB/ENR-50 (40/60)****(b) Morphology after melting at 185 °C****(vi) PHB/ENR-50 (30/70)****(vii) PHB/ENR-50 (40/60)**

Figure 1 Polarizing optical micrographs of PHB/ENR-50 blends: (a) as prepared samples, and (b) immediately after melting at 185°C.

ENR-50 blends subjected to heating at a rate of 20°C/min from 50 to 185°C and annealed or held at 185°C for one to two min.

RESULTS AND DISCUSSION

Morphology

The as formed solvent-cast membranes

Neat membranes of PHB/ENR-50 blends were obtained using solvent-casting technique. Visual inspection reveals transparent membranes of the 10/90 and 20/80 PHB/ENR-50 compositions and increasing opaqueness for membranes containing higher PHB,

namely 30/70, 40/60, 50/50, 60/40, 70/30, and 80/20. Figure 1(a) shows the optical micrographs of the as cast membranes. The compositions that show similar trend and do not offer new information are not shown here. In the composition range where ENR-50 is the major component, constituting the matrix with PHB as the dispersed phase, a fine and uniformly dispersed phase is observed for the 30/70 composition. A coarse dispersed phase appears in the 40/60 blend; while for 50/50 composition, it becomes fine and more closely packed again. In the case of 60/40 and 70/30 compositions, PHB, being the major component, forms the matrix of dense crystallites as the result of its highly crystalline nature. These morphologies are the results

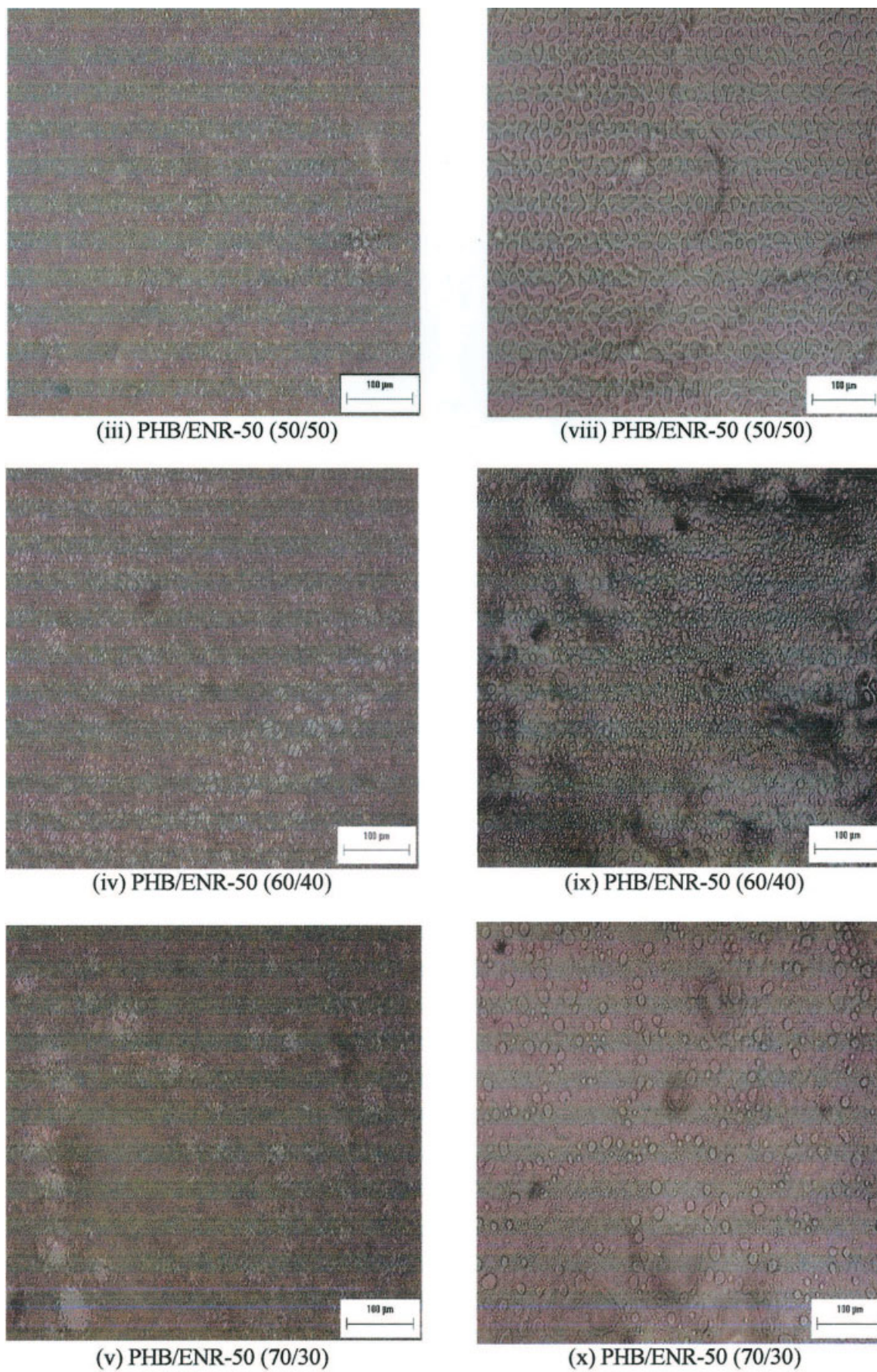


Figure 1 (Continued from the previous page)

of a rather complex process during the drying process. It is well known that crystalline polymer will crystallize from a solution when its concentration exceeds supersaturation point. We believe that in the present solvent cast PHB/ENR-50 blends, crystallization of PHB follows the same principle but in the presence of ENR, which becomes increasingly viscous and rubbery as the solvent evaporates. As a minor component, PHB crystallizes to form rigid dispersions of irregular shape embedded in the ENR matrix. By contrast, the flexible ENR will be dispersed as spherical droplets as PHB crystallizes to form rigid matrix.

The above features are evidence of a uniform phase distribution afforded by the solvent-casting technique, allowing optimum interfacial area crucial for the melt reaction. The DSC technique used in this study proves to be a useful tool as it allows precise control of the reaction conditions: heating, cooling, and isothermal annealing under nitrogen atmosphere.

The molten state

The melt reaction is presumably confined at the interfaces of the immiscible PHB and ENR-50 phases. To have a better insight, we investigated the melt morphology of the blends during annealing using polarizing optical microscope. Shown in Figure 1(b) are the optical micrographs of 30/70, 40/60, 50/50, 60/40, and 70/30 PHB/ENR-50 blends at 185°C, representing the melt phase morphologies of the respective blend compositions and showing characteristic interfaces where the reaction might occur. The micrographs were obtained using a 10× objective, limiting the visual examination to above ten microns. Based on careful observation during melting, the crystallites of PHB were seen to fuse and flow but confined within its domain. In most compositions, two-phase melt morphologies could be seen immediately after PHB has melted, featuring characteristic dispersions of one component in the matrix of the other. For example, while a single phase forms immediately upon melting of PHB crystallites for the 30/70 composition, stratified phases of PHB were observed for the 40/60 composition. In the 50/50 composition, however, the crystallites melt and form a continuous phase, characterizing a phase inversion phenomenon with ENR assuming a spherical dispersed phase. The size of the ENR-50 dispersed phase appears to decrease as the PHB content increases. It is interesting to note the complementary morphologies of 40/60 and 60/40 where PHB and ENR-50, both being the minor component, assume stratified and spherical phases, respectively. We could not see any inclusion of ENR-50 in the PHB dispersed phase in 40/60 composition or inclusion of PHB in the ENR-50 dispersed phase in the 60/40 composition. However, all the above two-phase morphologies disappear gradually, transforming completely into a single-phase melt after about one minute, a phenomenon that could be associ-

ated with the melt reaction. The same morphological trend is expected in the case of 30/70 and 70/30 compositions; unfortunately, the morphology of 30/70 melt could not be detected.

From these observations it may be summarized that the as formed membranes melt to give stratified phases of PHB when it constitutes the minor component as seen in the 40/60 composition, a phase-inversed morphology in the 50/50 composition, and spherical dispersions of ENR-50 when PHB constitutes the major component. Hence, one may say that the observed melt morphology is closely related to the morphology of the as formed membrane.

Isothermal melt reaction

This section discusses the characteristics of isothermal melt reaction in PHB/ENR-50 blends. The blends studied were exposed to the isothermal melt reaction procedure described in the experimental section. The results obtained and summarized below are direct evidence of the melt reaction, the principal interest in the present study of PHB/ENR-50 blends.

Figure 2 shows typical DSC traces of isothermal annealing at 190°C for 40/60, 50/50, and 60/40 compositions that represent the characteristic features of the melt reaction in PHB/ENR-50 blends in the temperature range studied, 184 to 199°C. Each trace exhibits an exothermic peak, indicating exothermic nature of the reaction. Broadening of peak with increasing PHB content suggests composition dependence of the reaction. Other compositions show a similar trend. Also shown in Figure 2 are the traces for neat PHB and ENR-50 samples prepared and annealed using the same conditions as for the blends. It is evident that neither endothermic nor exothermic peak was detected in PHB or ENR-50 although one might expect a heat of reaction associated with scission of the PHB chains. Thus, the observed heat of reaction in blends could only originate from reactions taking place during annealing. Figure 3 shows the DSC traces for 50/50 blend annealed at different temperatures.

Thus, the peak area corresponds to the heat of reaction, ΔH_r , which represents an average of the heats of reactions involved. The results obtained are summarized in Table II.

Figure 4 presents the heat of reaction and its dependence on the blend composition for two different temperatures, a typical feature observed for the melt reaction in the PHB/ENR-50 blends. The heats of reactions increase with PHB and ENR-50 as long as they remain as the dispersed phases respectively, and reach a maximum where the phase inversion might have presumably taken place. Analysis of data was carried out by formulating the heat of reaction, ΔH_r , as a function of PHB fraction:

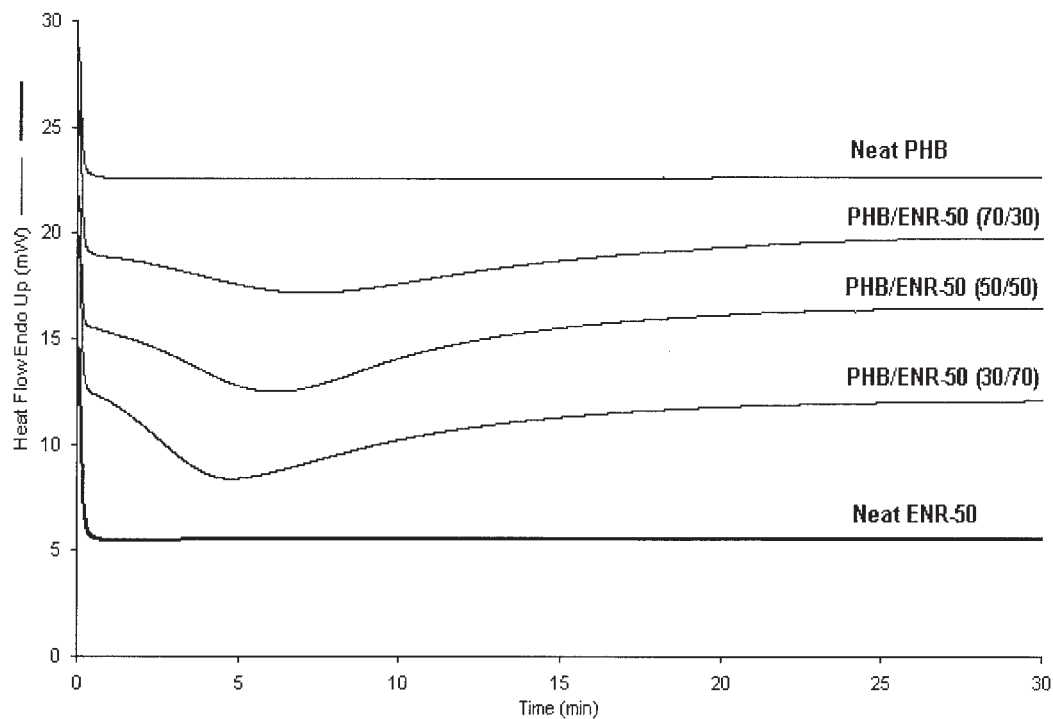


Figure 2 DSC traces of isothermal annealing at 190°C of neat PHB, neat ENR-50, and blends of PHB/ENR-50: 30/70, 50/50, and 70/30.

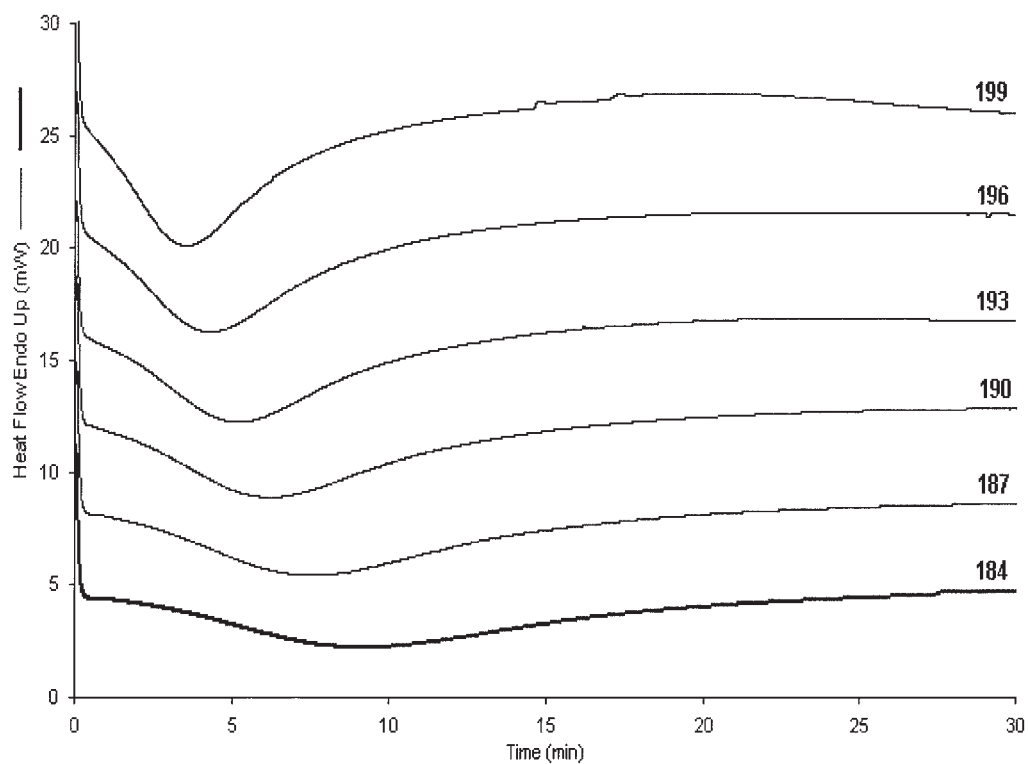


Figure 3 DSC traces of PHB/ENR-50 (50/50) blend at different temperatures.

TABLE II
Heats of Reactions, $t_{0.5}$, Center and $1/t_{0.5}$ of the Melt Reaction in PHB/ENR-50 Blends

Annealing temperature (°C)	ΔH_r (Jg ⁻¹)	$t_{0.5}$ (min)	$1/t_{0.5}$ (min ⁻¹)
30/70			
184	181 ± 1	8.31	0.12
187	199 ± 1	7.15	0.14
190	204 ± 8	5.82	0.17
193	195 ± 4	4.84	0.21
196	206 ± 4	4.28	0.23
199	204 ± 9	3.42	0.29
40/60			
184	201 ± 3	9.20	0.11
187	213 ± 9	8.63	0.12
190	234 ± 1	6.91	0.14
193	256 ± 5	6.09	0.16
196	220 ± 7	4.68	0.21
199	218 ± 7	3.72	0.27
50/50			
184	210 ± 7	9.77	0.10
187	213 ± 6	8.48	0.12
190	219 ± 1	6.74	0.15
193	218 ± 8	5.83	0.17
196	213 ± 8	4.77	0.21
199	218 ± 7	3.89	0.26
60/40			
184	178 ± 7	11.36	0.09
187	177 ± 9	9.16	0.11
190	176 ± 8	7.54	0.13
193	167 ± 5	6.29	0.16
196	179 ± 6	5.61	0.18
199	188 ± 9	4.52	0.22
70/30			
184	184 ± 9	11.20	0.09
187	196 ± 3	9.51	0.11
190	203 ± 14	8.19	0.12
193	196 ± 13	6.46	0.15
196	191 ± 5	5.97	0.17
199	206 ± 10	5.24	0.19

$$\Delta H = A\Phi^\alpha (1 - \Phi) \quad (1)$$

where Φ is the fraction of PHB (assuming $\Phi = w$), and the exponent α is associated with the nature of the reaction in a two-phase system; value of α is one for bulk reaction or one third for interfacial reaction. Alternatively, it can be also formulated by

$$\Delta H = \Delta H_{\max} \left(\frac{\Phi}{\Phi_{\max}} \right)^\alpha \left(\frac{1 - \Phi}{1 - \Phi_{\max}} \right) \quad (2)$$

where,

$$\Phi_{\max} = \frac{\alpha}{\alpha + 1} \text{ and } \Delta H_{\max} = A\Phi_{\max}^\alpha (1 - \Phi_{\max}) \quad (3)$$

Eqs. (1) and (2) are completely equivalent. Equation (1) allows determination of parameters A and α from the log plots of $[\Delta H/(1 - \Phi)]$ versus Φ whose values are

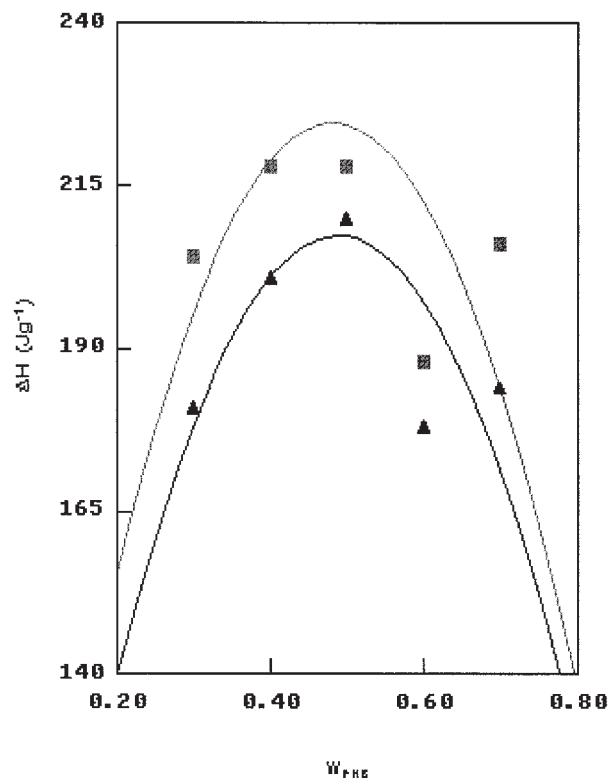


Figure 4 Plot of heat of reaction versus PHB content in PHB/ENR-50 blends: (▲) 184°C, and (■) 199°C.

in turn used to calculate Φ_{\max} , and ΔH_{\max} and to generate the best regression curves (average correlation around 0.96). The best curves for 184 and 199°C as typical examples are shown in Figure 4. Table III summarizes the results for the temperatures studied.

Interestingly, α is independent of temperatures and fluctuates around an average value of 0.9, suggesting that the melt reaction is a bulk reaction. This is unexpected, though, because the reaction in the present immiscible PHB/ENR-50 blend system is reckoned to be restricted at the interfaces. Φ_{\max} is independent of temperature, with an average value of 0.5, which is characteristic of a symmetric composition dependence of the heat of reaction. ΔH_{\max} does not systematically vary with temperatures. The results also suggest that phase inversion occurs in the blends with PHB content between 45 to 50%, in good agreement with the mor-

TABLE III
Heats of Reactions; Summary of α , Φ_{\max} , ΔH_m

T/°C	A/Jg ⁻¹	α	Φ_{\max}	ΔH_{\max} /Jg ⁻¹	r
184	799	0.95	0.49	207	0.981
187	793	0.88	0.47	216	0.955
190	801	0.84	0.46	225	0.931
193	767	0.80	0.45	223	0.884
199	847	0.92	0.49	224	0.962

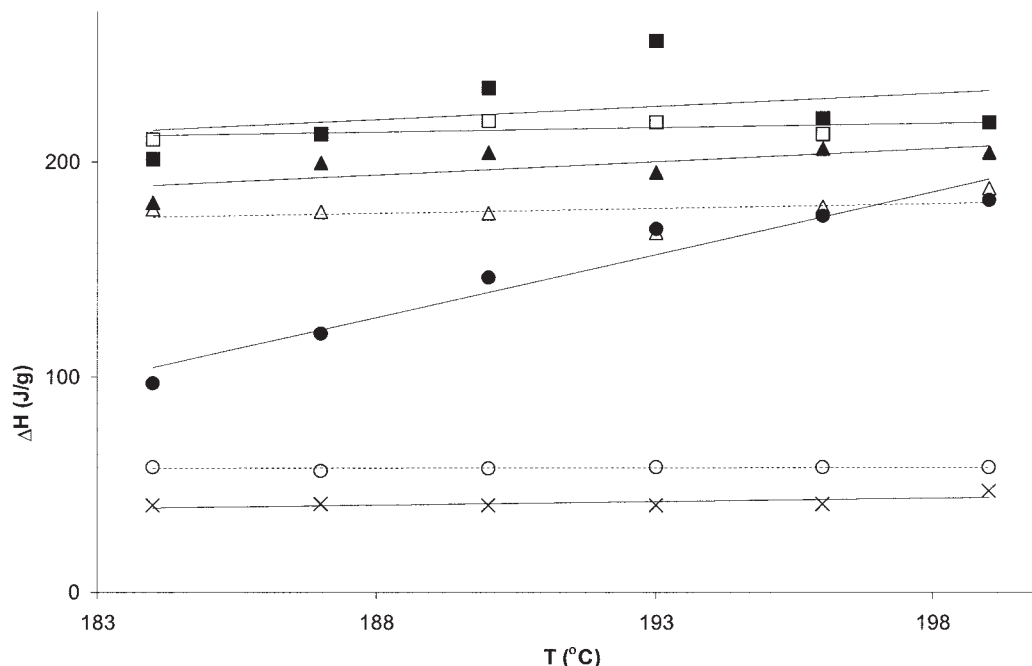


Figure 5 Plot of heat of reaction versus temperature for PHB/ENR-50 blends: (×) 10/90, (●) 20/80, (▲) 30/70, (■) 40/60, (□) 50/50, (△) 60/40, and (○) 80/20; (—) PHB content 40% and below, and (---) PHB content 50% and above.

phological behavior observed earlier. Nevertheless, as can be seen in Figure 5, the heats of reactions increase with temperature for blends containing below 50% PHB and remain independent of temperature above 50% PHB.

The reaction half-time, $t_{0.5}$, and the overall rate of reaction

Broadening of the exothermic peaks of the DSC traces with descending temperatures is an indication of a slowing down of the overall rate of reaction. This is another feature that allows a kinetic parameter, the half-time of the melt reaction, to be determined from the traces. The ratio of the peak area at time t and the total peak area determined by integration of the peak of the trace (details are described in the reaction kinetics) gives a normalized extent of the melt reaction. The time at 50% extent of reaction corresponds to the half-time of the reaction, $t_{0.5}$. To a good approximation, the reciprocal of half-time, $1/t_{0.5}$, gives a measurement of the overall rate of the reaction. The results are summarized in Table II. The overall rate of reaction increases with temperature is shown in Figure 6.

Reaction mechanism

We begin the discussion on the kinetics of the melt reaction with a proposal of the reaction mechanism as given in Scheme 1.

The melt reaction starts with a random thermal scission of long chain PHB molecules to shorter chains bearing carboxyl ends according to reaction (1), where the reactivity depends on the average chain length and decreases exponentially with reaction time.^{11,12} Reactions between the epoxide group of ENR and carboxyl group of various carboxylic acids have been reported where the reactivity was observed to increase with decreasing pKa value of the acids.^{3,4} In the presence of ENR, as in the present PHB/ENR-50 blend system, reaction (1) would immediately be followed by reaction (2), the ring opening of the epoxide groups that present in the vicinity of the newly formed carboxyl groups. Subsequent to this ring opening reaction, the hydroxyl group is thus formed and, being reactive towards both the carboxyl and epoxide groups, may trigger reactions (3) and (4), respectively. They may also be in competition with each other. Taking into consideration the effect of steric hindrance, one can easily understand that reaction (4) may be the most hindered, (2) the least hindered, while reaction (3) is in between. Evidence of reaction (3) in the present system could be seen from a slight decrease in solubility of annealed samples since it leads to crosslinking of the ENR chains. One may therefore generalize that reactions (1) and (2) dominate the melt reaction, while enabling reaction (3) and others to take place accordingly, though with less significance. As for the consumption of the carboxyl group, only reactions

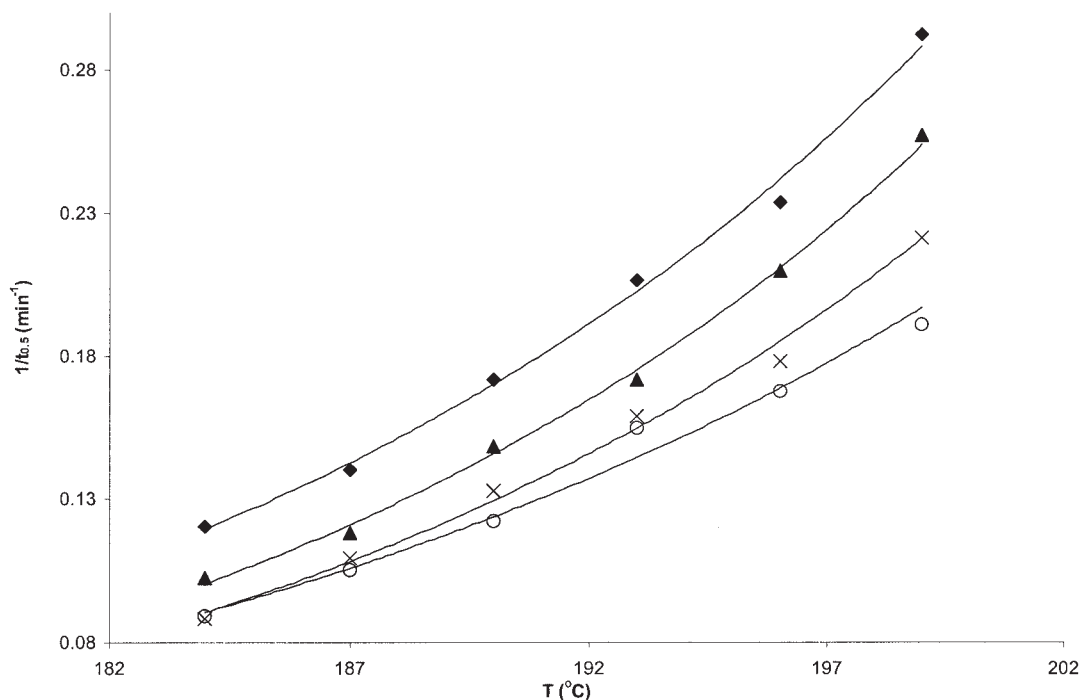


Figure 6 Plot of $1/t_{0.5}$ versus T for different blend compositions: (◆) 30/70, (▲) 50/50, (×) 60/40, and (○) 70/30.

(2) and (3) are assumed to be important in the analysis of experimental kinetic data.

The reaction kinetics

Integration of the peak of the DSC trace associated with isothermal reaction shown in Figure 2 allows determination of normalized degree of conversion as a function of time, $z(t)$. This quantity is defined as the ratio of the peak area at time t and the total peak area.

Typical plots of $z(t)$ as a function of time t for different reaction temperatures are shown in Figure 7. A similar feature is observed for different blend compositions at 190°C as shown in Figure 8.

In the following discussion we present the analysis of $z(t)$ to obtain several kinetic parameters that characterize the melt reaction based on the proposed reaction steps in Scheme 1. We must note that the degradation of neat PHB could not be detected from the DSC trace. This means that the exothermic traces observed for the blends are due to reactions (1), (2), and probably (3), that constitute the melt reaction. Hence, the function $z(t)$ describes the normalized extent of the melt reaction as a function of time. Based on the proposed mechanism, we present a simplified model for the purpose of kinetic analysis. It comprises the thermal degradation of PHB of certain average chain length, X , in the presence of ENR to shorter chains bearing reactive carboxyl end-group, Y , according to reaction (1). Y is subsequently consumed in the ring opening reaction with the epoxide group of ENR ac-

ording to (2) and may undergo esterification according to reaction (3) to form the final products, that is, ENR grafted with PHB chains, Z . X is a quantity associated with the average chain length of the PHB molecules, an important parameter that influences the reactivity of degradation¹¹⁻¹². The DSC traces obtained allow kinetic analysis of PHB degradation in blends, although in its neat form does not reveal any evidence as mentioned earlier. In the discussion that follows, we term the former degradation process as the decay of PHB, to differentiate it from thermal degradation of neat PHB.

The simplified model may be approximated by a serial reaction scheme of the type,

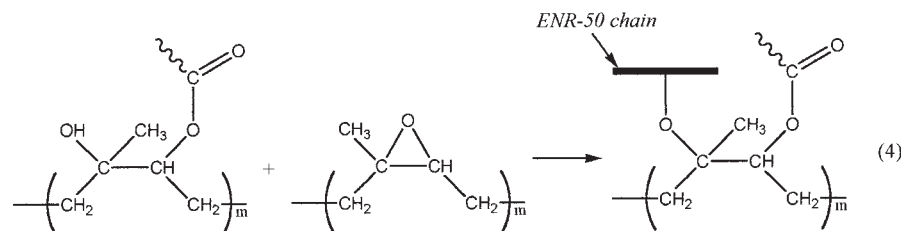
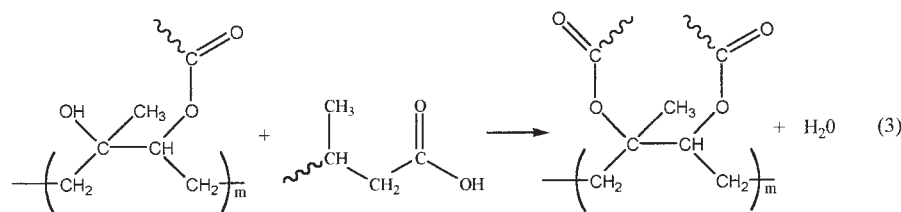
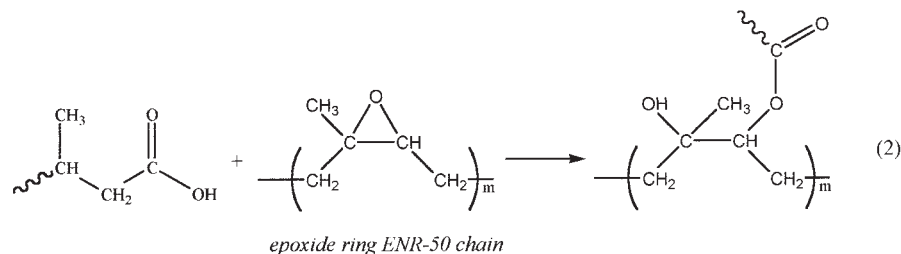
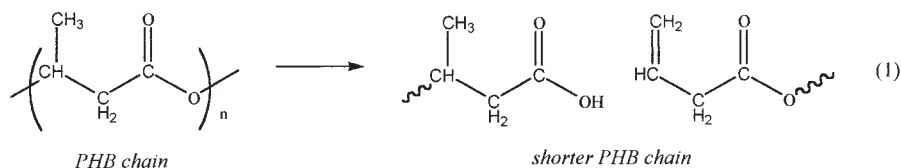


where k is the rate constant for PHB decay and k' the rate constant for carboxyl consumption reactions. The formation of Z from X via Y is accompanied with an overall heat of reaction, which is recorded as the DSC trace.

To derive the rate expression, we use normalized quantities of X , Y , and Z , symbolized by x , y , and z , respectively. For the first step, that is, the decay of PHB, we assume the rate as

$$\frac{dx}{dt} = -knt^{n-1}x \quad (5)$$

which for $x = 1$ at $t = 0$ resolves to give



Scheme 1 Reaction mechanisms of PHB/ENR-50 melt blends.

$$x = \exp(-k'/n t)^n \quad (6)$$

$$\frac{dz}{dt} = k' y \quad (9)$$

Quantities k , n , and t are rate constant (min^{-n}), exponential constant, and time (min), respectively.

For the second step, that is, the consumption of carboxyl group, Y , we have the rate as

$$-\frac{dy}{dt} = k' y + x' \quad (7)$$

The first term represents the consumption of Y with the rate constant k' (min^{-1}), whereas the second term equals the rate of production of Y , that is, $x' = dx/dt$. The solution to eq. (7) with $y = 0$ at $t = 0$ is

$$y = -e^{-k't} \int_0^t x' e^{k't} dt \quad (8)$$

The third rate equation is simply

The solution to eq. (9) is simply $x + y + z = 1$ with $z = 0$ at $t = 0$. Hence, we have

$$z = 1 + e^{-k't} \int_0^t x' e^{k't} dt - x \quad (10)$$

From eq. (10) one can easily show that

$$-\ln(1 - z) = \left(\frac{t}{\tau}\right)^n - \ln[1 - e^{k'tn-k't} \int_0^t x' e^{k't} dt] \quad (11)$$

Eventually, the form that is useful for evaluation of $z(t)$ may be recast from eq. (11) as

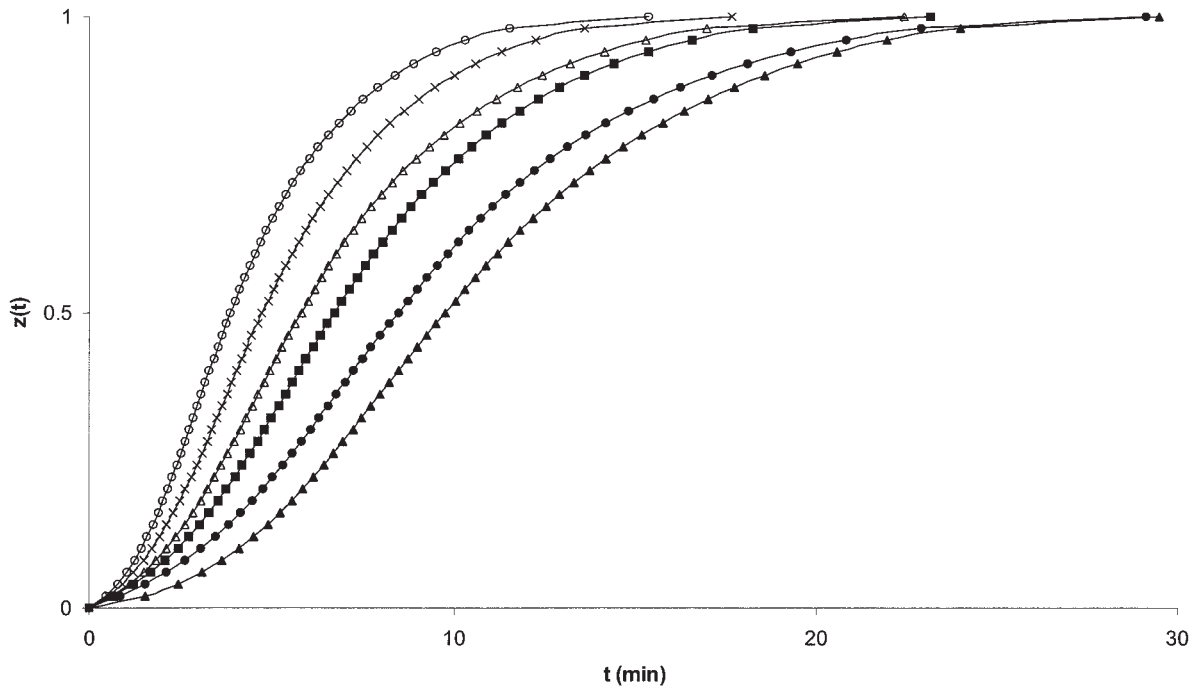


Figure 7 Plot of $z(t)$ versus t of PHB/ENR-50 (50/50) blend at different temperatures ($^{\circ}\text{C}$): (▲) 184, (●) 187, (■) 190, (△) 193, (×) 196, and (○) 199.

$$-\ln(1-z) = k't - \ln\left[1 + k' \int_0^t e^{k't - kt^n} dt\right] \quad (12)$$

a) For $t \rightarrow \infty$, Eq. (12) reduces to

$$-\ln(1-z) = k't - \ln[\text{const.}] \quad (13)$$

Evaluation of the kinetic parameters required consideration of two situations in terms of eq. (12).

b) For $t \rightarrow 0$, Eq. (12) reduces to

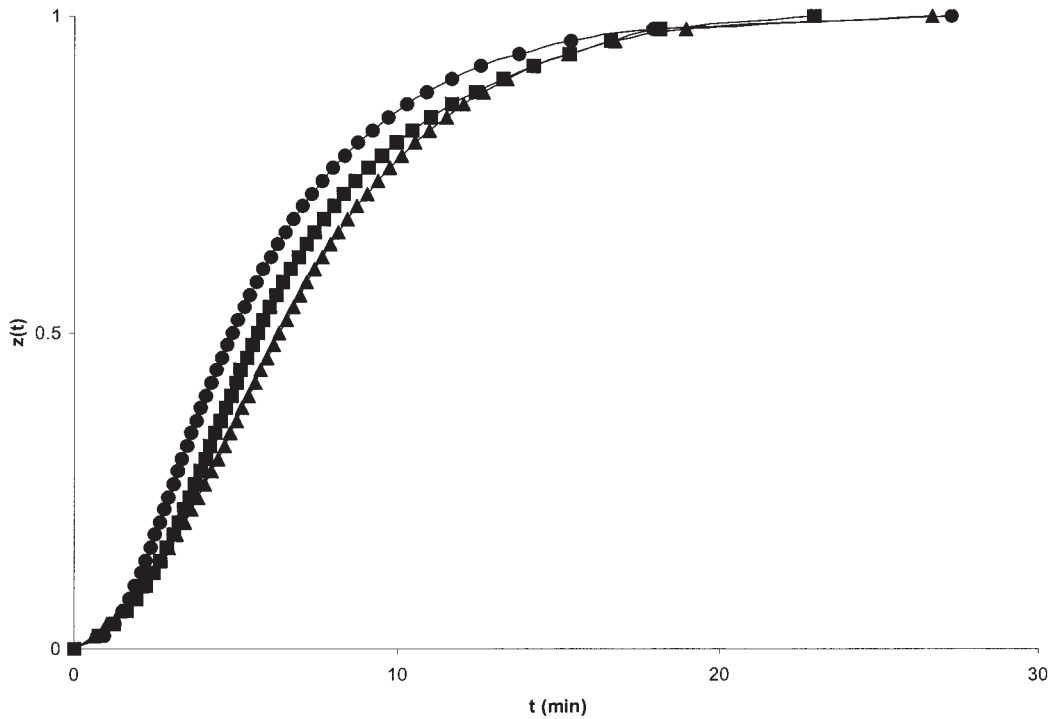


Figure 8 Isotherms of PHB/ENR-50 blends at 190°C : (●) 30/70, (■) 50/50, and (▲) 70/30.

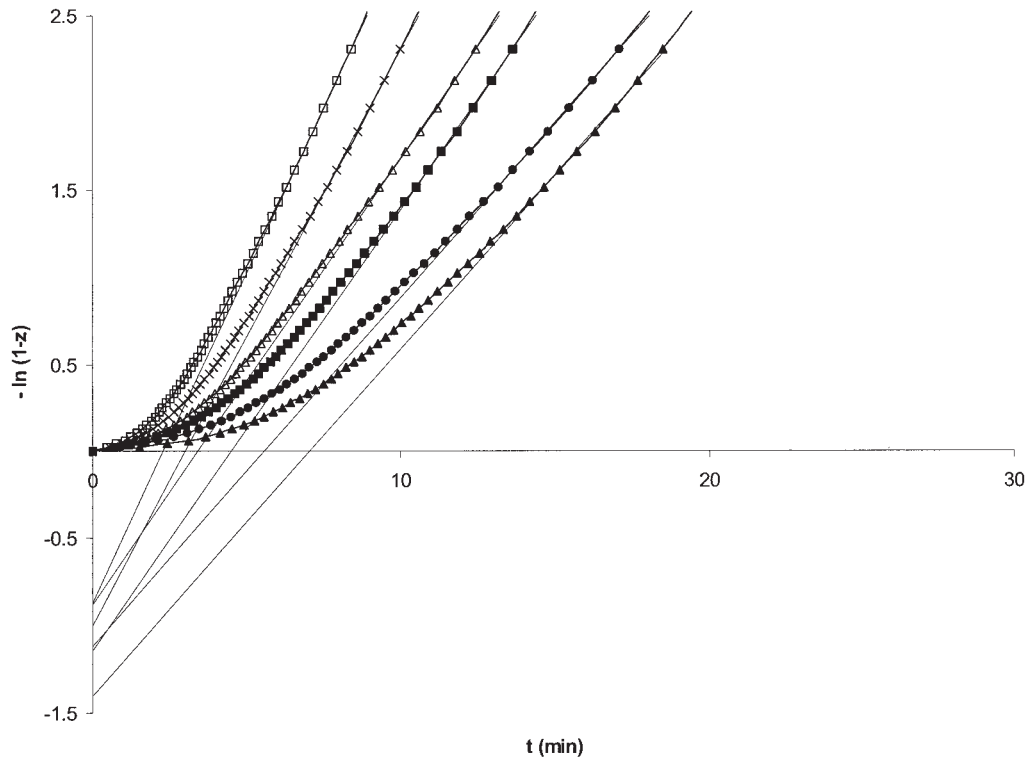


Figure 9 Plot of $-\ln(1-z)$ versus t of PHB/ENR-50 (50/50) blend at different temperatures ($^{\circ}\text{C}$): (\blacktriangle) 184, (\bullet) 187, (\blacksquare) 190, (\triangle) 193, (\times) 196, and (\square) 199.

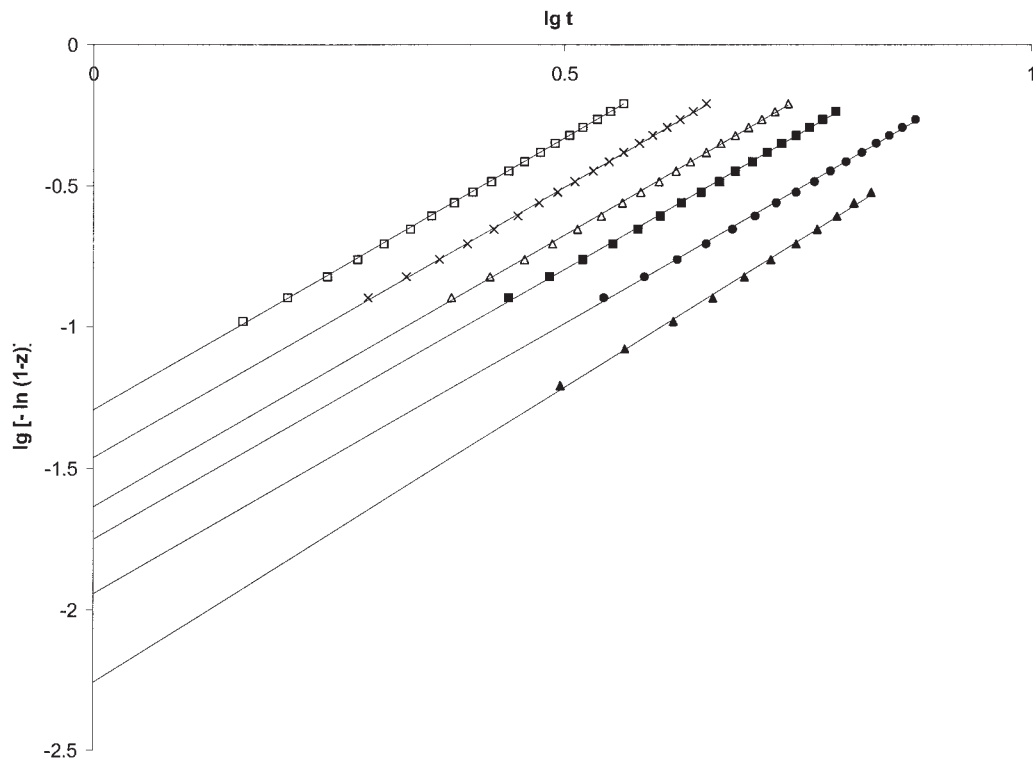


Figure 10 Plot of $\lg[-\ln(1-z)]$ versus $\lg(t)$ of PHB/ENR-50 (50/50) blend at different temperatures ($^{\circ}\text{C}$): (\blacktriangle) 184, (\bullet) 187, (\blacksquare) 190, (\triangle) 193, (\times) 196, and (\square) 199.

TABLE IV
Summary of the Kinetic Quantities, k' , k , and n

Annealing temperature (°C)	k' (min ⁻¹)	k (min ⁻ⁿ)	n
30/70			
184	0.16	0.30	0.94
187	0.17	0.36	0.91
190	0.20	0.47	0.79
193	0.26	0.53	0.81
196	0.27	0.61	0.78
199	0.36	0.73	0.82
40/60			
184	0.16	0.26	1.00
187	0.14	0.30	0.97
190	0.17	0.36	0.96
193	0.20	0.42	0.90
196	0.27	0.53	0.88
199	0.39	0.66	0.95
50/50			
184	0.20	0.27	1.09
187	0.20	0.30	0.91
190	0.25	0.38	0.91
193	0.26	0.42	0.93
196	0.33	0.52	0.92
199	0.38	0.62	0.92
60/40			
184	0.16	0.23	0.99
187	0.18	0.28	0.88
190	0.22	0.34	0.87
193	0.27	0.40	0.99
196	0.28	0.44	0.90
199	0.31	0.54	0.82
70/30			
184	0.15	0.23	0.89
187	0.16	0.27	0.83
190	0.20	0.32	0.83
193	0.24	0.40	0.79
196	0.27	0.43	0.81
199	0.27	0.48	0.77

$$-\ln(1-z) = \left(\frac{k'k}{n+1} - \frac{k'^2}{2} t^{1-n} \right) t^{n+1} \quad (14)$$

If we make an approximation of eq. (14) by assuming $n \approx 1$, then

$$-\ln(1-z) = \left(\frac{k'k}{n+1} - \frac{k'^2}{2} \right) t^{n+1} \quad (15)$$

According to eq. (15) the term $-\ln(1-z)$ follows a power law for small t .

Equations (13) and (15) enable us to evaluate the experimental data, $z(t)$, and determine the kinetic parameters k , k' , and n . Plot of $[-\ln(1-z)]$ versus t clearly reveals that the experimental data obey eq. (12). Typical plots are shown in Figure 9. By extrapolation to $t = 0$, values of k' and $\ln[\text{const.}]$ were calculated from the slope and the intercept, respectively. Figure 10 shows the log plot of eq. (15) where n and k were determined from the slope and the intercept, respectively. Table IV

summarizes the kinetic quantities n , k' , and k . This approach gives k and k' corresponding to the initial stage and the infinite stage of the reaction scheme.

The dependence of k on composition, shown in Figure 11(a), reveals an increase with increasing ENR content and a decrease with increasing PHB content. However, the rate constant k' does not show any systematic composition dependent as shown in Figure 11(b). The experimental values of n are to a good approximation close to 1 suggesting that the melt reaction in PHB/ENR-50 blends follows a first order kinetics. Using $n \approx 1$ allows one to express the experimental $k(\text{min}^{-n}) \approx k(\text{min}^{-1})$ and apply it for the rest of our discussion and analysis.

We also evaluate the reliability of the expressions and accuracy of the quantities. Assuming $n = 1$ and integrating the second term of eq. (12) one obtains an expression for the intercept in terms of k' and k , as

$$-\ln(1-z) = -\ln\left(1 - \frac{k'}{k' - k}\right) \quad (16)$$

We also obtained an expression relating the half-time, k , and k' according to eq. (13) as

$$\ln 2 = k' t_{0.5} - \ln\left(1 - \frac{k'}{k' - k}\right) \quad (17)$$

Using eqs. (16) and (17) and the parameters listed in Table III, one can calculate the theoretical intercept and half-time and compare them with the experimental values. As an example, we summarize the results for 30/70 PHB/ENR-50 in Table V.

Generally, we found reasonable agreement between experimental and calculated values with deviations not exceeding 10%. We recognize that the present approximation based on the serial reaction scheme to obtain eqs. (12), (13), and (15) is certainly a simplified model. The parameters could be determined more precisely if one is able to determine the function $x = x(t)$, as in eq. (6), experimentally for degradation of neat PHB using DSC technique, which unfortunately could not be detected. Nevertheless, the above analysis allows determination of kinetic parameters k , k' , and n that characterize the melt reaction in the PHB/ENR-50 blends.

Temperature dependence

The temperature dependence of parameters k and k' are analyzed according to the Arrhenius equation. Figure 12 shows typical plots of $\ln k$ and $\ln k'$ versus $1/T$, respectively, where linear relationships having reasonably good correlations are observed. The results obey satisfactorily the Arrhenius equation as follows,

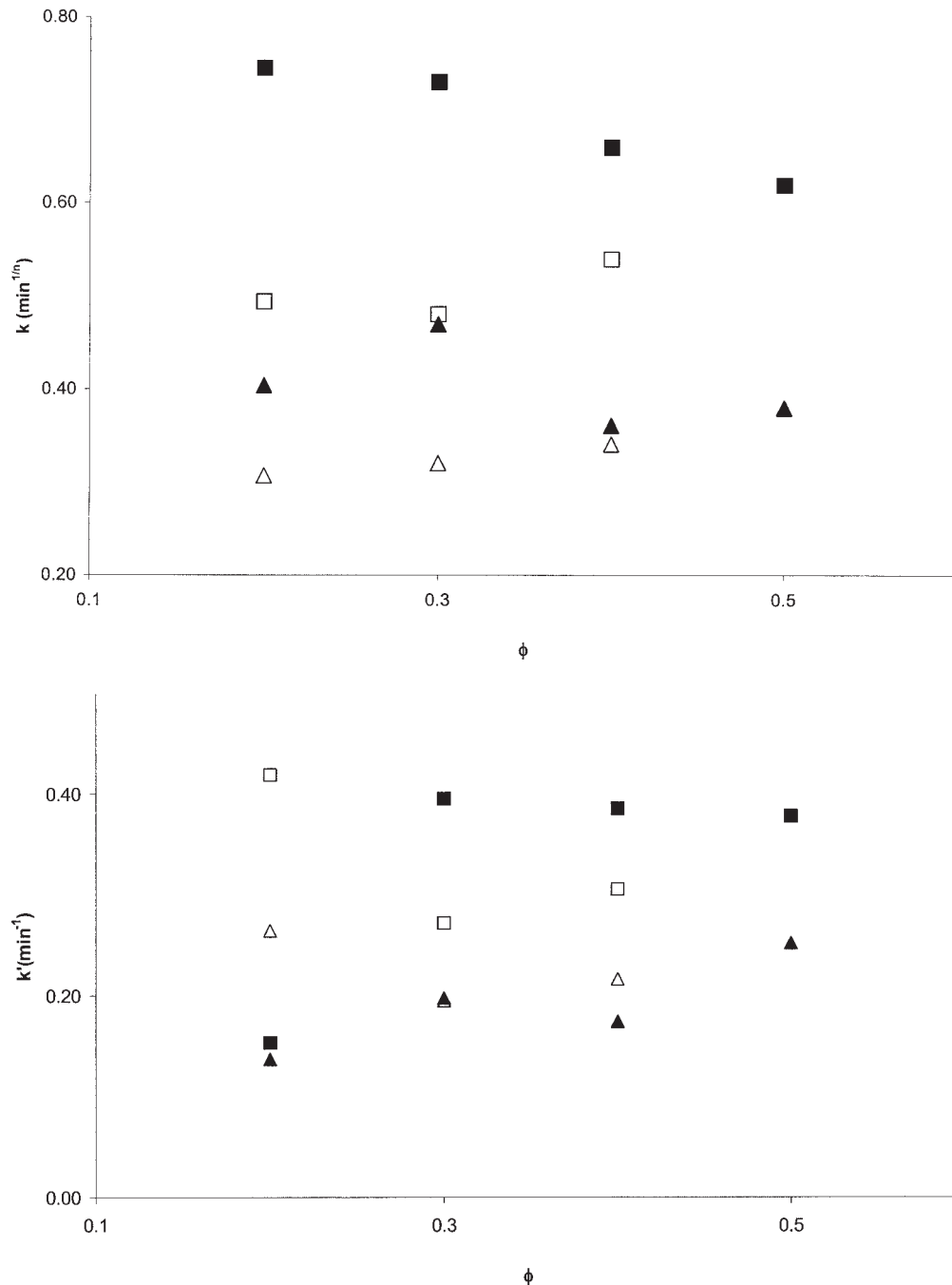


Figure 11 (a) Plot of k versus weight fraction of dispersed phase: PHB as dispersed phase (▲) 190°C, and (■) 199°C; ENR-50 as dispersed phase (△) 190°C, and (□) 199°C; (b) Plot of k' versus weight fraction of dispersed phase: PHB as dispersed phase (▲) 190°C, and (■) 199°C; ENR-50 as dispersed phase (△) 190°C, and (□) 199°C.

$$k = k_o \exp\left(-\frac{E_k}{RT}\right) \text{ and } k' = k'_o \exp\left(-\frac{E_{k'}}{RT}\right) \quad (18)$$

The activation energies E_k and $E_{k'}$ characterizing the melt reaction are summarized in Table VI. The energies are not symmetrical with respect to composition. For melt reaction to occur, it has to overcome higher energy barrier in the blend with lower PHB content

TABLE V
Kinetic Parameters of the Melt Reaction
for 30/70 PHB/ENR-50 Blend

Temp (°C)	k' (min ⁻¹)	k (min ⁻ⁿ)	n	intercept	$t_{0.5}$ (min)		
184	0.16	0.30	0.94	-0.68	*-0.76	9.5	*8.6
190	0.20	0.47	0.79	-0.54	-0.55	6.5	6.2
199	0.36	0.73	0.82	-0.51	-0.68	4.0	3.6

* Calculated values.

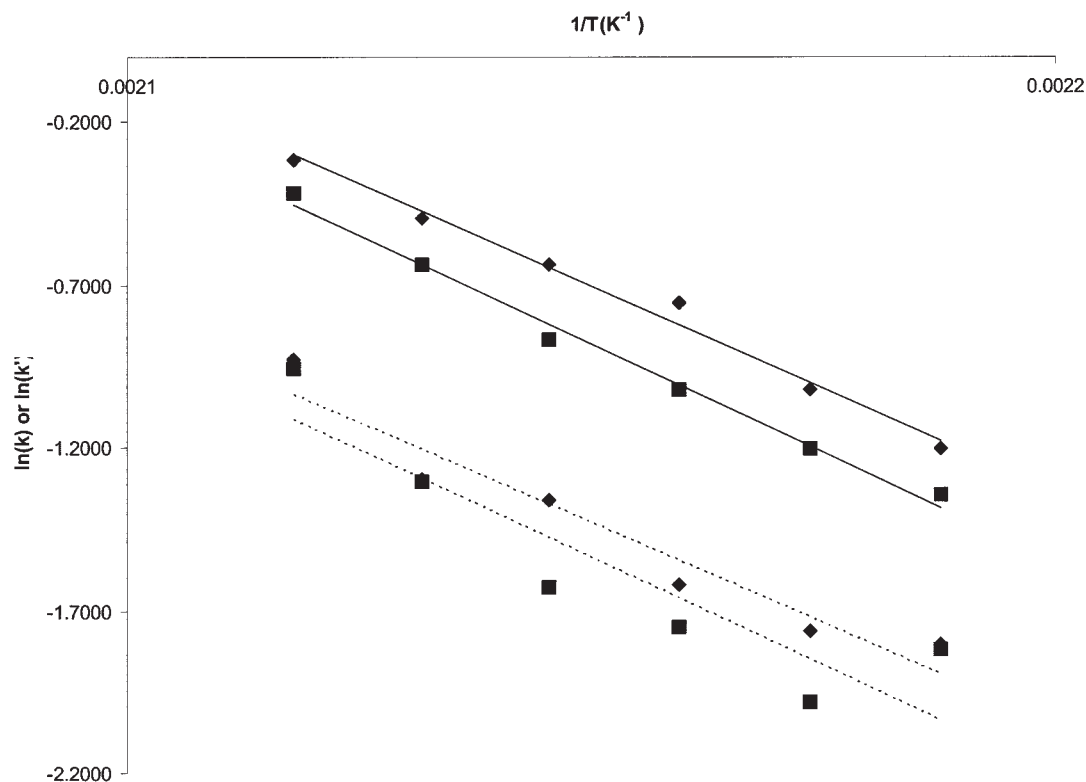


Figure 12 Plot of $\ln(k')$ and $\ln(k)$ versus $1/T$ for different composition of PHB/ENR-50 blends: (\blacklozenge) 30/70, and (\blacksquare) 40/60; (—) $\ln(k)$ versus $1/T$, and (---) $\ln(k')$ versus $1/T$.

(PHB the dispersed phase) than that of complementary blend with higher PHB content.

Comparison of experimental $E_{k'}$ values with the activation energy of the reactions between the epoxide of ENR and several carboxylic acids reported in literatures using DSC technique⁴ shows that they fall within the range as reported for the reaction of stearic acid, 87.16kJ/mol, and dichloroacetic acid, 115.96kJ/mol, respectively. This may suggest that the reactivity of ring opening reaction in PHB/ENR-50 blends is influenced by acidity of degraded PHB. Experimental values of E_k for decay of PHB in blend with ENR-50 are lower than that for degradation of pure PHB, 212kJ/mol, as reported by Kunioka et al. obtained using DSC technique.¹² This suggests that the reactiv-

ity is much higher for PHB in blend with ENR-50 than in its pure state. Thus, the presence of epoxide group may have promoted degradation of PHB. We also compare the decay rate constant of PHB in 30/70 blend, $k = 4.7 \times 10^{-1} \text{min}^{-1}$ (assuming $n \approx 1$), and the degradation rate constant of pure PHB, $k_d = 1.4 \times 10^{-4} \text{min}^{-1}$,¹² both measured at 190°C, and note that the decay reaction of PHB in blend with ENR-50 is faster than the degradation of neat PHB. This is consistent with the observed reactivity between PHB decay in blend with ENR and degradation in neat PHB.

Glass transition temperature

Figure 13 shows the DSC traces for 50/50 blend obtained after subjecting the sample to the glass transition temperature thermal treatment. This composition is selected because it gives significant response and is presented here as evidence in support of the melt reaction. Two separate T_g s at 1.2 and -18.4°C corresponding to that of PHB and ENR-50, respectively, are observed after annealing the blend at 190°C for one minute. After four minutes of annealing, a significant inwards shift of the T_g s at -6.2 and -16.8°C for PHB and ENR-50, respectively, is observed. They apparently merged to become a single transition at -14.1°C after annealing for eight minutes. These results show

TABLE VI
Summary of $E_{k'}$ and E_k

PHB/ENR-50 (wt %)	$E_{k'}$ (kJ/mol)	r'	E_k (kJ/mol)	r
20/80	11	0.9780	83	0.9607
30/70	103	0.9660	105	0.9942
40/60	110	0.9114	111	0.9954
50/50	81	0.9699	101	0.9949
60/40	80	0.9807	99	0.9960
70/30	81	0.9824	91	0.9905
80/20	100	0.9920	101	0.9969

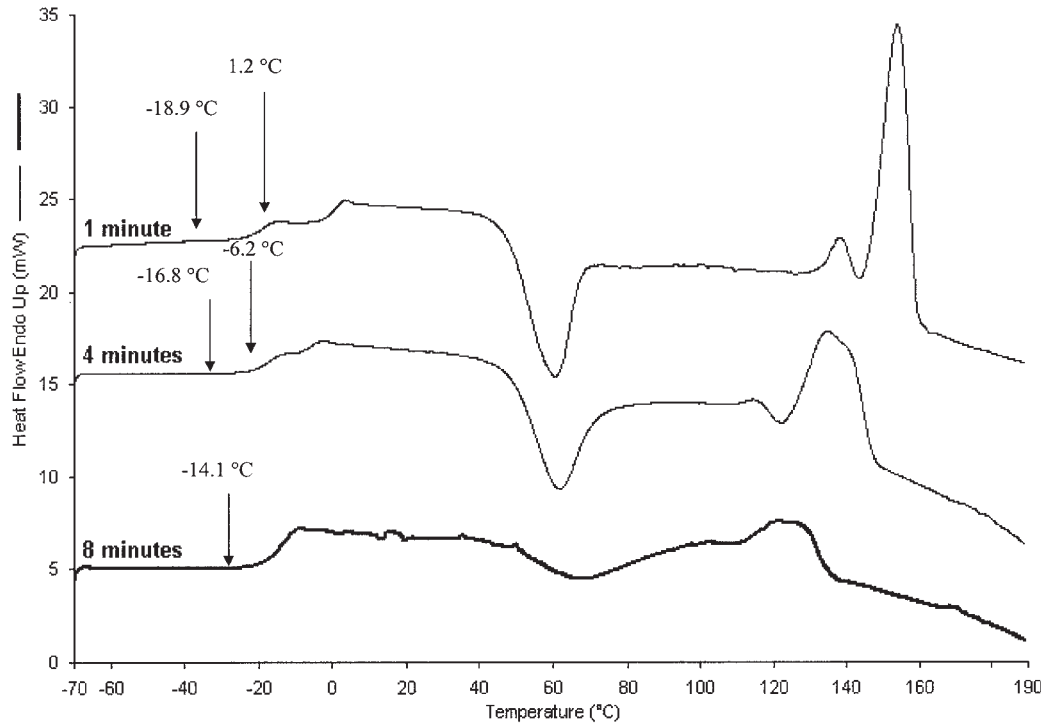


Figure 13 DSC traces of PHB/ENR-50 (50/50) blend obtained after glass transition temperature thermal treatment.

that increasing annealing time lead to a progressive shift of the glass transition temperatures of PHB and ENR-50 towards each other. The shift indicates progressive change in compatibility in the PHB/ENR-50 blends. This effect is attributed to reaction at the in-

terfaces as proposed in Scheme 1. Reactions (2) and (3) and the consequential grafting of PHB chains onto the ENR-50 backbone might be responsible for the shift.

Also evident from the DSC traces are the effects of melt reaction on cold crystallization and melting be-

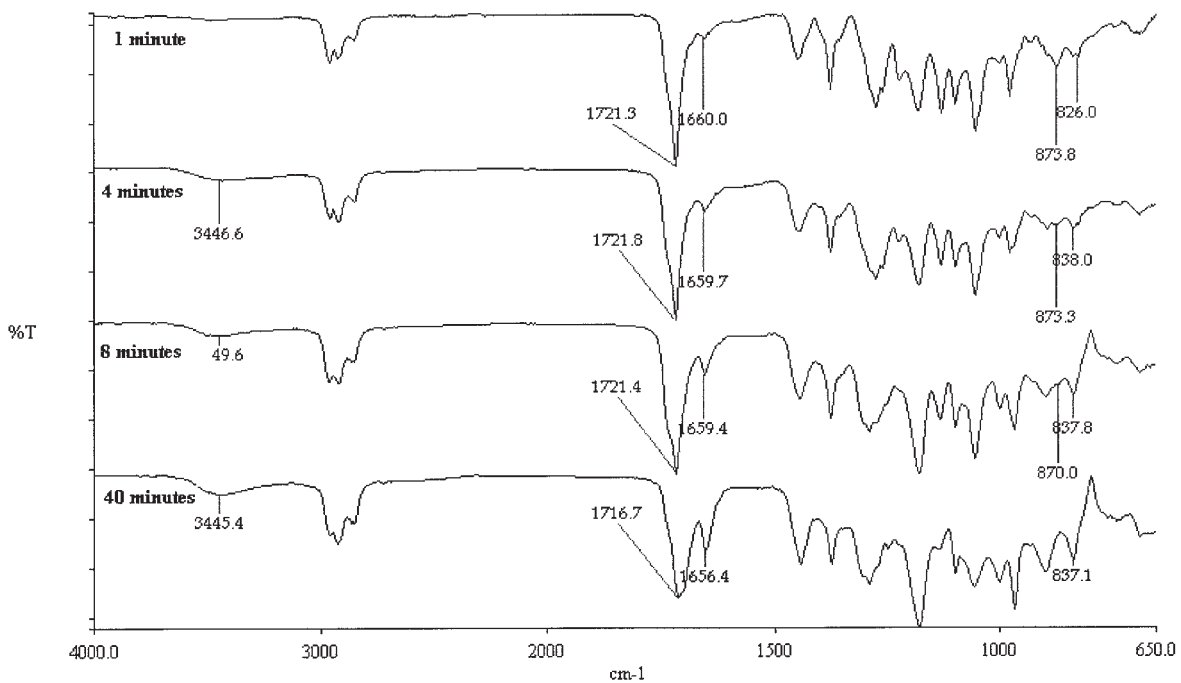


Figure 14 FTIR spectrum for PHB/ENR-50 (30/70) blend after glass transition temperature thermal treatment.

havior of PHB in the blend. The degree of cold crystallization and the melting temperature apparently decreases with increasing annealing time. These phenomena are attributed with the effects of the structural change brought about by reactions (2) and (3).

We must also note here that the time taken for the two T_g s to merge into a single transition after annealing at 190°C is about eight minutes while the time taken for the reaction to complete at 190°C is about twenty minutes (DSC traces in Fig. 3). Although a single glass transition is observed, it does not necessarily mean that the melt reaction is complete. One would expect that the crystallization and melting behavior of PHB would also be affected by the above structural change. Further discussion related to these matters is not intended here as study is still underway.

FTIR spectroscopy

The FTIR spectra obtained for 30/70 PHB/ENR-50 at different annealing times are shown in Figure 14. This particular blend composition gave strong signals characteristic of ENR-50, probably due to it being the major component, and is presented here as more evidence of the melt reaction in the PHB/ENR-50 blends. The band of interest is 873 cm^{-1} associated with the epoxide group; its intensity decreases as the annealing time is increased, apparently diminished after eight minutes. The results confirm the ring opening reaction involving the epoxide group. The band at 1721 cm^{-1} is associated with the carbonyl of PHB and that of the ester group associated with new graft linkages but does not show significant change in its intensity. The bands at 1656 cm^{-1} and 836 cm^{-1} are associated with the double bond of ENR-50 where addition of the double bond chain ends of decomposed PHB reaction (1) might have contributed to the apparent increase in their intensities with annealing time.

CONCLUSION

This study has revealed the physical and chemical characteristics featuring the melt reaction in immiscible blends of PHB and ENR-50 prepared by solvent-casting technique. The melt morphologies of PHB/ENR-50 blends show stratified PHB phases in the 40/60 blend, spherical dispersions ENR-50 phases in the 60/40 composition, and a phase inversion in the

50/50 composition. All the observed two-phase morphologies of the melt are unstable, presumably due to the melt reaction. The melt reaction in PHB/ENR-50 blends has been shown to occur during isothermal annealing in the temperature range 184 to 199°C using DSC technique. The heat of reaction increases with the increase in PHB and ENR-50 content as long as they remain the dispersed phases and exhibits a maximum around 45 to 50% PHB. Other experimental evidence including the melt morphologies, glass transition temperatures, and the FTIR spectra confirmed the occurrence of the melt reaction.

Kinetic analysis based on the melt reaction comprises degradation of PHB, and consumption of the carboxyl group allows the reaction to be modeled in terms of a serial reaction scheme. It enables derivation of a function $z(t)$ that describes, to a good approximation, the formation of grafted PHB in terms of normalized enthalpy as a function of time, determined from the exothermic peak of the DSC trace. Further equations are derived from the $z(t)$ function by applying the limiting conditions and approximations and subsequently using their respective graphical plots to determine the kinetic parameters that characterize the melt reaction in the PHB/ENR-50 blends.

The authors gratefully acknowledge financial support from Universiti Sains Malaysia (the Short Term Grant No. 304/P.Kimia/634066).

References

1. Morikawa, H.; Marchessalut, R. H. *Can J Chem* 1981, 59, 2306.
2. Baker, C. S. L.; Gelling, L. R.; Newell, R. *Rubber Chem Technol* 1985, 58, 67.
3. Derouet, D.; Brosse, J. C.; Tillekeratne, L. M. K. *J Nat Rubb Res* 1990, 5, 296.
4. Copeland, J. K.; Thames, S. F. *J of Coat Technol* 1994, 66, 833, 59.
5. Pillin, I.; Pimbert, S.; Feller, J. F.; Levesque, G. *Polymer Engineering and Science* 2001, 41, 178.
6. Avella, M.; Martuscelli, E. *Polymer* 1991, 29, 1731.
7. Chee, M. J. K.; Ismail, J.; Kummerlowe, C.; Kammer, H. W. *Polymer* 2002, 43, 1235.
8. Avella, M.; Martuscelli, E.; Orsello, G.; Raimo, M.; Pascucci, B. *Polymer* 1997, 38, 6135.
9. Yam, Y. M.; Ismail, J.; Kammer, H. W.; Lechner, M. D.; Kummerlowe, C. *Polymer* 2000, 41, 9073.
10. Khaw, C. B.; Ismail, J. Thermal behavior of PHB/ENR-50 blends (Final year undergraduate project report); Universiti Sains Malaysia, 2002; p 23.
11. Chan, C. H. Ph.D. thesis, Universiti Sains Malaysia, 2002; p 38.
12. Kunioka, M.; Doi, Y. *Macromolecules* 1990, 23, 1933.